

# A high-resolution genomic and phenotypic analysis of resistance evolution of an *Escherichia coli* strain from a critically unwell patient treated with piperacillin/tazobactam

Alice J. Fraser<sup>1</sup>, Robert Ball<sup>2</sup>, Daire Cantillon<sup>1</sup>, Laura E. Brettell<sup>3,4</sup>, Fabrice E. Graf<sup>5</sup>, John T. Munnoch<sup>6</sup>, Paul A. Hoskisson<sup>6</sup>, Joseph M. Lewis<sup>2,5,7</sup>, Jon J. van Aartsen<sup>2,8</sup>, Christopher M. Parry<sup>5,9</sup>, Eva Heinz<sup>3,5,6,\*†</sup> and Thomas Edwards<sup>1,\*†</sup>

## Abstract

**Introduction.** Resistance to the  $\beta$ -lactam/ $\beta$ -lactamase inhibitor (BL/BLI) combination antibiotic piperacillin/tazobactam (TZP) predominantly occurs via  $\beta$ -lactamase enzymes, also leading to resistance to third-generation cephalosporins (3GCs). However, if  $\beta$ -lactamases inactive against 3GCs and inhibited by tazobactam are expressed at high levels, leading to enzyme hyperproduction, the surplus enzyme escapes inhibition by tazobactam and inactivates the antibiotic piperacillin.

**Hypothesis/Gap statement.** Understanding this mechanism is clinically relevant, as enzyme hyperproduction can emerge upon antibiotic administration, resulting in treatment failure despite initial resistance profiles supporting TZP use.

**Aim.** Our aim was to determine whether this was a case of within-patient evolution and by what mechanism or an acquisition of a second unrelated, more resistant, strain.

**Methodology.** Whole-genome sequencing was performed on the isolate to determine the genetic basis of resistance. We also assessed the impact of TZP exposure on the amplification of the  $bla_{TEM-1}$  gene and monitored the stability of gene copy number over 5 days in the absence of antibiotic pressure. In addition, we determined the MICs of ceftriaxone and TZP, with TZP MIC contextualized in relation to gene copy number and resistance levels.

**Results.** We report the identification of an *Escherichia coli* isolate that developed resistance to TZP during patient treatment but maintained sensitivity to ceftriaxone. We show that TZP resistance evolved via IS26-mediated duplication of a  $bla_{TEM-1}$  containing transposable unit on a plasmid, resulting in hyperproduction of TEM-1  $\beta$ -lactamase, and that ten copies of  $bla_{TEM-1}$  induce resistance greater than 32 times the MIC. Furthermore, under experimental conditions, exposure to TZP further increases amplification of  $bla_{TEM-1}$ , whereas, in the absence of TZP, gene copy number of IS26 and  $bla_{TEM-1}$  remains stable over 5 days, despite a 48,205 bp genome size increase compared to the pre-amplification isolate. We additionally detect phenotypic changes that might indicate host adaptation potentially linked to the additional genes that are amplified.

**Conclusion.** Our analysis advances the understanding of infections caused by isolates evolving  $\beta$ -lactamase hyperproduction, which represents a complex problem in both detection and treatment. As 40% of antibiotics active against WHO priority pathogens in the pre-clinical pipeline are BL/BLI combinations, further investigations are of urgent concern.

Received 18 December 2024; Accepted 03 May 2025; Published 19 May 2025

**Author affiliations:** <sup>1</sup>Department of Tropical Disease Biology, Liverpool School of Tropical Medicine, Liverpool, L3 5QA, UK; <sup>2</sup>Liverpool Clinical Laboratories, Liverpool University Hospitals NHS Foundation Trust, Liverpool, L7 8XP, UK; <sup>3</sup>Department of Vector Biology, Liverpool School of Tropical Medicine, Liverpool, L3 5QA, UK; <sup>4</sup>School of Science, Engineering and Environment, University of Salford, Manchester, M5 4WT, UK; <sup>5</sup>Department of Clinical Sciences, Liverpool School of Tropical Medicine, Liverpool, L3 5QA, UK; <sup>6</sup>Strathclyde Institute of Pharmacy and Biomedical Sciences, University of Strathclyde, Glasgow, G4 0RE, UK; <sup>7</sup>Department of Clinical Infection, Microbiology and Immunology, University of Liverpool, Liverpool, L69 3BX, UK; <sup>8</sup>Department of Microbiology, NHS Dumfries and Galloway, Dumfries and Galloway Royal Infirmary, Cargenbridge, Dumfries, DG2 8RX, UK; <sup>9</sup>Alder Hey Children's NHS Foundation Trust, Liverpool, L12 2AP, UK.

\*Correspondence: Eva Heinz, eva.heinz@strath.ac.uk; Thomas Edwards, Thomas.Edwards@lstm.ac.uk

**Keywords:** antimicrobial resistance;  $\beta$ -lactam;  $\beta$ -lactamase; enzyme hyperproduction; *Escherichia coli*; gene amplification; IS26; TEM-1.

**Abbreviations:** ANI, average nucleotide identity; AST, antimicrobial susceptibility testing; BL/BLI,  $\beta$ -lactam/ $\beta$ -lactamase inhibitor; CA-MHB-2, cation-adjusted Mueller Hinton broth; ESBLs, extended-spectrum  $\beta$ -lactamases; 3GCs, third-generation cephalosporins; LB, Luria-Bertani; LCL, Liverpool Clinical Laboratories; LPD, dihydroliipoamide dehydrogenase; ONT, Oxford Nanopore Technologies; qPCR, quantitative PCR; RGI, resistance gene identifier; SNPs, single nucleotide polymorphisms; TZP, piperacillin/tazobactam; TZP-R, TZP-resistant; TZP-R/3GC-S, TZP-resistant/3GC-susceptible; TZP-S, TZP-susceptible; WGS, whole-genome sequencing.

†These authors contributed equally to this work

Fifteen supplementary figures and one supplementary table are available in the online Supplementary Material.

002018 © 2025 The Authors



This is an open-access article distributed under the terms of the Creative Commons Attribution License. This article was made open access via a Publish and Read agreement between the Microbiology Society and the corresponding author's institution.

## DATA AVAILABILITY

All sequence data can be found at the Sequence Read Archive bioproject ID PRJNA1061590, which includes short- (Illumina) and long-read (ONT) data for the sensitive (SRR27502767 and SRR27502765, respectively) and the resistant isolate (SRR27502766 and SRR27502764, respectively) as well as the assemblies (GCA\_037070795.1, GCA\_037070775.1).

## INTRODUCTION

The spectrum of clinical disease caused by *Escherichia coli* infections ranges from uncomplicated localized infections, such as those affecting the lower urinary tract, to disseminated and serious infections, including bacteraemia. In the case of infections which result in patient hospitalization, antimicrobials belonging to the  $\beta$ -lactam class are often used as an empirical treatment, primarily due to their broad spectrum of activity and safe use [1]. Cephalosporins, especially third-generation cephalosporins (3GCs), such as cefotaxime, ceftazidime and ceftriaxone, are  $\beta$ -lactams suitable for treating suspected sepsis, pneumonia and meningitis [2]. In cases where the patient is critically ill or a resistance to 3GCs is likely, carbapenems such as ertapenem, imipenem or meropenem may be used. These antimicrobials are generally considered antimicrobials of ‘last resort’, beyond which treatment options are limited [3]. Pathogenic *E. coli* strains are now often resistant to early generations of  $\beta$ -lactam drugs, primarily due to the production of  $\beta$ -lactamase enzymes, acquired via mobile genetic elements. Extended-spectrum  $\beta$ -lactamases (ESBLs), which have increased hydrolytic capability and can break down 3GCs, are increasingly prevalent in *E. coli* globally and lead to treatment failures of common first- and second-line agents. Collectively, these put our ability to provide effective treatments at risk, and in 2019, over 250,000 deaths worldwide were attributed to antimicrobial-resistant *E. coli* infections [4].

To address the increase in infections caused by drug-resistant,  $\beta$ -lactamase-producing *E. coli* strains, the combination of a  $\beta$ -lactamase inhibitor with a  $\beta$ -lactam antibiotic is a common strategy used to restore clinical efficacy. The hydrolytic activity of the  $\beta$ -lactamase is countered by the binding of the inhibitor to the enzyme, thus leaving the antibiotic free to exert its bactericidal activity and render isolates de facto susceptible.

Piperacillin/tazobactam (TZP) is a clinically important  $\beta$ -lactam/ $\beta$ -lactamase inhibitor (BL/BLI) combination therapy, indicated for the first-line empirical treatment of serious infections, including those escalating to bacteraemia and caused by *E. coli* [5]. Tazobactam, a ‘suicide inhibitor’, irreversibly binds to the  $\beta$ -lactamase present, rendering it inactive and thus restoring the activity of piperacillin, a penicillin  $\beta$ -lactam class antibiotic. Tazobactam has *in vitro* activity against Ambler class A and Ambler class C  $\beta$ -lactamases, which include AmpC, TEM, SHV and CTX-M enzymes, is well tolerated and, combined with piperacillin, has broad-spectrum activity against both Gram-negative and Gram-positive pathogens [6].

The introduction of TZP as a treatment option, however, has rapidly been followed by observations of resistant strains. Mechanisms which reduce susceptibility to TZP may be independent of  $\beta$ -lactamase production, such as increased drug efflux due to efflux pump overexpression [7]; decreased influx due to porin downregulation [8]; mutations in penicillin-binding proteins, leading to reduced binding of the penicillin [9]. Alternatively, production of multiple  $\beta$ -lactamases [10], which can enable the bacteria to overcome the inhibitory effects of tazobactam via saturation of the inhibitor, or production of carbapenemases [11], to which tazobactam lacks activity, may permit  $\beta$ -lactamase hydrolysis of the penicillin.

In some strains, selective resistance to TZP occurs, whilst susceptibility to 3GCs is retained. This can be induced by hyperproduction of enzymes which would otherwise be blocked by tazobactam, but the increased production means excess enzymes can thus escape the inhibitor and function as normal. The other cause of this phenotype can be mutations in enzymes which would otherwise not induce TZP resistance. In *E. coli*, different resistance mechanisms have evolved which induce hyperproduction of TEM and SHV enzymes. These include mutations in promoter regions [12], gene duplication events [13–15] and an increase in plasmid copy number [16]. Alternatively, the acquisition of CTX-M-15 enzyme variants exhibiting the S133G mutation can induce selective resistance to TZP [17]. The TZP-resistant/3GC-susceptible (TZP-R/3GC-S) phenotype is not restricted to particular *E. coli* clones and has been reported in a wide range of sequence types [18]. Selecting an appropriate treatment for these strains can be challenging. Whilst treatment with a 3GC could be effective and would reduce exposure to antimicrobials of last resort, TZP treatment failure can also be indicative of ESBL or high-level AmpC production [19]. Carbapenem use may therefore be considered by some clinicians as a safer option to ensure successful treatment is not further delayed [20].

Here we report the characterization of a clinical *E. coli* strain isolated from blood culture, which evolved resistance during treatment of a patient with TZP, resulting in the emergence of the previously described TZP-R/3GC-S phenotype. Using whole-genome sequencing (WGS) and subsequent bioinformatic analyses, combined with *in vitro* laboratory investigations, we describe the cause of the resistance phenotype: an extensive gene amplification of  $bla_{\text{TEM-1}}$  resulting in  $\beta$ -lactamase hyperproduction. We also highlight extensive duplication of additional non-antimicrobial resistance genes alongside  $bla_{\text{TEM-1}}$ , which has not previously been described. Finally, we observed that whilst successful treatment included carbapenems, the use of 3GC may have also been suitable and thus prevented the use of an antimicrobial of last resort.

## METHODS

### Bacteria isolates, storage and media

Clinical *E. coli* isolates were grown from blood cultures performed at Liverpool Clinical Laboratories (LCL) on the day of admission and day 5 post-admission. Isolates were stored in glycerol broth in Microbank tubes (Pro-lab Diagnostics, UK) at  $-80^{\circ}\text{C}$  and resurrected from glycerol stocks on Luria–Bertani (LB) agar (Sigma, UK) at  $37^{\circ}\text{C}$  for 18 h. Single colonies were then picked and used for subsequent experiments.

Control strains of *Bacteroides thetaiotaomicron* (VPI-5482) and *Pseudomonas aeruginosa* (NCTC 13437) were used as positive controls in our anaerobic growth assay and for the assay assessing biofilm formation, respectively.

Both were resurrected from glycerol stocks and grown on brain heart infusion agar (Sigma) supplemented with  $5\text{ mg l}^{-1}$  of haemin (Sigma) and LB agar, respectively.

### Antimicrobial susceptibility testing

Initial antimicrobial susceptibility testing (AST) at LCL was performed using the disc diffusion method according to EUCAST guidelines. Susceptibility to 3GCs was inferred from cefpodoxime. Upon receipt, we verified the TZP phenotypes where the susceptible isolate was susceptible to TZP (MIC  $1\text{--}2/4\text{ }\mu\text{g ml}^{-1}$ ) and the resistant isolate was resistant (MIC  $256\text{--}512/4\text{ }\mu\text{g ml}^{-1}$ ) to TZP via broth microdilution, according to the guidelines as set out by EUCAST [21], which states the clinical breakpoint as  $8/4\text{ }\mu\text{g ml}^{-1}$  [22]. Ceftriaxone susceptibility was also carried out according to the same guidelines, with a clinical breakpoint of  $\geq 2\text{ }\mu\text{g ml}^{-1}$  indicating resistance. Piperacillin and tazobactam (both Sigma, UK) were solubilized in DMSO (Sigma) to a stock concentration of  $10\text{ mg ml}^{-1}$  and then sterilized through a  $0.22\text{ }\mu\text{m}$  polyethersulfone filter unit (Milipore, USA). Ceftriaxone was solubilized in sterile molecular grade water to a final concentration of  $1\text{ mg ml}^{-1}$  and stored at  $-20^{\circ}\text{C}$  as single use aliquots. Triplicate liquid cultures were grown from the selection of three distinct colonies, and each liquid culture was then tested in triplicate.

### Extraction of DNA for WGS and quantitative PCR

Single colonies were transferred to 10 ml of LB broth (Sigma, UK) and grown overnight at  $37^{\circ}\text{C}$ , 200 r.p.m. Long fragments of genomic DNA, used for Oxford Nanopore Technologies (ONT) sequencing, were extracted using the Masterpure™ Complete DNA and RNA Purification Kit (Lucigen, UK), following the manufacturer's instructions for the purification of DNA from cell samples. Short-fragment DNA, used for Illumina sequencing and quantitative PCR (qPCR), was extracted using the DNeasy™ Blood and Tissue Kit (Qiagen, Germany), following the protocol for Gram-negative bacteria. The quality and size of the short-fragment DNA used for Illumina sequencing were assessed using the TapeStation (4,150) system and the DNA ScreenTape Kit (Agilent, USA). All genomic DNA used for sequencing was quantified using the Qubit Fluorometer with the dsDNA BR Kit (Invitrogen, USA).

### Whole-genome sequencing

Short-read sequencing was performed by Microbes NG (Birmingham, UK) using their in-house 250 bp paired-end protocol. Long-read sequencing was performed on a MinION MK1B sequencing device (ONT, UK). Library preparation was carried out according to the manufacturers' protocol, using the ligation sequencing kit (SQK-LSK109) and Native Barcoding Expansion Kits (EXP-NBD104; all ONT). Sequencing was carried out using a FLOW-MIN106 R9.4.1 flow cell (ONT); the libraries were loaded as a pool containing ten sample libraries in total.

### Assemblies

The generated fastq files then underwent trimming using Trimmomatic (v0.39) [23], with a sliding window quality cut-off value of Q20, and were quality assessed using FASTQC (v0.11.9) [24].

Basecalling and de-multiplexing of long reads were performed with Guppy (v5.0.7) [25], using the super-accurate model for basecalling. Long-read sequences were then filtered using Filtlong (v0.2.1) [26] and adapters trimmed using Porechop (v0.2.4) [27].

Long-read-first hybrid assemblies were produced using Unicycler (v0.5.0) [28] with the Miniasm+Racon pipeline; these were then visualized using Bandage (v0.8.1) [29] before being polished with long reads using Medaka (v1.5.0) [30]. Assemblies then underwent polishing with short reads using Polypolish (v0.5.0) [31] and NextPolish (1.4.1) [32]. Finally, polished assemblies were quality checked using the bwa-mem (v0.7.17) [33] and samtools (v1.9) [34] to map reads back to the consensus assembly sequence. These were then visualized using Artemis (v18.2.0) [35] and the Artemis comparison tool (v18.2.0) [36].

### Genome analyses

Polished assemblies were annotated using PROKKA (v1.14.5) [37]; any unannotated genes of interest were manually queried using BLAST. Sequence type was determined using the Achtman [38] scheme for multi-locus sequence typing (v2.0), serotype was determined by SerotypeFinder (v2.0) [39] and the average nucleotide identity (ANI) of the chromosomal genomes was calculated using the OrthoANiU algorithm [40]. Plasmid replicons were determined using PlasmidFinder (v2.0.1) [41], and

mobile genetic elements and resistance genes were identified using ResFinder (v4.1) [42] and resistance gene identifier (RGI) (v6.0.1), using the CARD (v3.2.6) [43] database. Finally, single nucleotide polymorphisms (SNPs) and indels were identified using breseq (v0.31.1) [44].

### Nitrocefin assay

Overnight cultures of the isolates were normalized to an OD at 600 nm ( $OD_{600}$ ) of 0.1 in 10 ml of LB broth and centrifuged at 4,500 g for 15 min. The supernatant was discarded, and the pellet resuspended in 5 ml of PBS. The resuspension was then sonicated on ice for three intervals of 15 s, with a 30 s break between each sonication, using a Soniprep 150 plus (MSE centrifuges, UK). Briefly, 90  $\mu$ l of the supernatant was added to 10  $\mu$ l of a 0.5 mg ml<sup>-1</sup> nitrocefin solution in a 96-well clear, flat-bottom plate. The absorbance of the plate was read at  $OD_{450}$  every 39 s for 9 min and 45 s, using a FLUOstar OMEGA spectrophotometer (BMG lab systems, Germany). Triplicate overnight liquid cultures were grown from three distinct colonies, each selected from the TZP-susceptible (TZP-S) and the TZP-resistant (TZP-R) isolates. Each culture was then assayed in triplicate.

### In vitro passage of isolates in TZP and determination of *bla*<sub>TEM-1</sub> and IS26 copy number

When comparing the bacterial isolates in the absence of TZP, the isolates were grown overnight at 37 °C in LB broth. Triplicate overnight liquid cultures were grown from three distinct colonies, each selected from the TZP-S and the TZP-R isolates, which then underwent DNA extraction and subsequent qPCR.

To investigate gene copy number in the presence of increasing concentrations of tazobactam or piperacillin, bacterial isolates were grown in cation-adjusted Mueller Hinton broth (CA-MHB-2) containing either tazobactam fixed at 4  $\mu$ g ml<sup>-1</sup> and increasing concentrations of piperacillin or piperacillin fixed at 8  $\mu$ g ml<sup>-1</sup> and increasing concentrations of tazobactam. AST using the broth microdilution method was then undertaken as per EUCAST guidelines [21]. If growth was observed visually in the well, the culture underwent DNA extraction and subsequent qPCR. For each concentration of TZP, three biological repeats were performed, using cultures which were grown from distinct colonies derived from a glycerol stock stored at -80 °C.

Bacterial isolates were also grown over a period of 5 days, and the gene copy number was assessed at each 24 h time point. Single colonies were grown in CA-MHB-2, CA-MHB-2 containing 4  $\mu$ g ml<sup>-1</sup> of tazobactam and 256  $\mu$ g ml<sup>-1</sup> piperacillin and M9 liquid media (prepared as described in the supplementary methods, but without agar), for 24 h at 37 °C, 200 r.p.m. Following 24 h incubation, cultures were vortexed and 1  $\mu$ l transferred to fresh media. This process was repeated over a period of 5 days, and following each 24 h incubation, 1 ml of culture was removed, which then underwent DNA extraction and subsequent qPCR. For each isolate and media combination, three biological repeats were performed following inoculation with distinct colonies which were grown from a glycerol stock stored at -80 °C.

### Quantitative PCR

Change in gene copy number of *bla*<sub>TEM-1</sub> and IS26 was determined using the  $\Delta\Delta CT$  method for relative quantification [45] when compared to a single copy of the *uidA* housekeeping gene. The QuantiTect<sup>®</sup> SYBR Green PCR master mix (Qiagen, Germany) was used, following the manufacturer's instructions. Primers used to detect *bla*<sub>TEM-1</sub>, IS26 and *uidA* were as previously described [13, 46, 47]. Primers used to detect *repA* can be found in the supplementary methods. All primers were added to the reaction at a final concentration of 400 nM.

### Statistical analysis

Statistical analyses were performed in R studio with R (v4.1.1) [48] using the R Stats (v4.1.1) and DescTools (v0.99.48) packages. Pairwise comparisons of means between two groups used t-tests, and more than two groups used ANOVA, with Dunnett's post-hoc test used for pairwise group comparisons where ANOVA identified a significant between-group difference [ttest(), DunnettTest() and aov() functions] as indicated for the respective experiments in the corresponding figure legends. Graphs were produced using ggplot2 (v3.4.2) [49]. Diagrams of the amplified genomic region were created using gggenes (v0.5.0) [50] and Clinker (v0.0.28) [49, 51].

## RESULTS

### Clinical case summary

In January 2022, a woman in her 80s was admitted to the Royal Liverpool University Hospital with a suspected disseminated bacterial infection. Blood tests on admission showed a raised white cell count and raised C-reactive protein level (Fig. S1, available in the online Supplementary Material), and subsequent clinical diagnoses were community-acquired pneumonia, pyelonephritis and infective discitis (Fig. S2).

Upon admission, the patient was immediately started on a combination of antimicrobial therapy, which included TZP. The blood culture from the day of admission resulted in the growth of *E. coli* resistant to amoxicillin but susceptible to cefpodoxime,

ciprofloxacin, gentamicin, meropenem and TZP. The patient remained clinically unwell, and on day 5, another blood culture was obtained, which resulted in the growth of *E. coli* with the same resistance profile except TZP, to which the *E. coli* was now resistant. The patient was then successfully treated with a sequential regimen of meropenem, ertapenem and ciprofloxacin. An extended clinical case summary can be found in the supplementary information.

### Characterization of the isolates and identification of resistance mechanisms

We confirmed the phenotypic resistance profiles to TZP as susceptible (MIC=1–2/4 µg ml<sup>-1</sup> for TZP-S) and resistant (MIC=256–512/4 µg ml<sup>-1</sup> for TZP-R). Both isolates were also confirmed as sensitive to ceftriaxone (MIC≤0.25 µg ml<sup>-1</sup> for TZP-S and TZP-R). The growth curves (supplementary methods) of the two isolates under standard conditions showed no significant difference (Fig. S3).

Assembling the short- and long-read sequencing data resulted in a total genome length of 5,305,542 bp for the TZP-S isolate (GCA\_037070795.1). This included one conjugative plasmid 162,475 bp in length which was assembled as a single contig and contained IncFIA, IncFIB and IncFII replicons. The assembly of the TZP-R isolate (GCA\_037070775.1) resulted in a total genome length of 5,353,725 bp and included a larger conjugative plasmid (assembled as one contig) of 210,651 bp and which contained the same replicons as the TZP-S isolate. Also assembled within the TZP-R genome was an additional smaller circular DNA molecule of 54,316 bp; however, due to a lack of sequencing depth of both long and short reads, we could not confidently ascertain the structure of this region. A plasmid replicon was not detected within this molecule, and it was not predicted to contain any antimicrobial resistance genes (ARGs), though it was predicted to contain a single copy of *ompX*, an outer membrane porin, along with multiple copies of *IS21*, an exonuclease, and phage-related assembly and integrase genes.

We determined the isolates to belong to sequence type 131 and serotype O153:H4. We also confirmed the clonality of the TZP-S and TZP-R isolates, as the ANI of the chromosomal genomes was calculated as 99.99% and only three SNPs were detected between them on the chromosome. Genome assemblies of both isolates revealed the presence of the  $\beta$ -lactamase *bla*<sub>TEM-1</sub>; however, whilst only one copy of the gene was assembled in the TZP-S isolate (Fig. 1a), ten copies were assembled in the TZP-R isolate (Fig. 1c). In both cases, *bla*<sub>TEM-1</sub> was located on the large conjugative plasmid, as part of a transposable unit (Fig. 1b) that contained a transposase gene, along with *dosP*, *merE*, *merD* and *lpd1*. In addition, a hypothetical protein, which when manually queried was described as a ‘mobile element protein’, and *pinE*, which encodes a site-specific DNA recombinase, were also annotated only once in the transposable unit of both the TZP-S and TZP-R isolates. These were not duplicated. In both the TZP-S and TZP-R isolates, the transposable unit contained flanking copies of *IS26*, which were oriented in opposing directions. The *IS26* elements located within the duplicated region in the TZP-R isolate were oriented in the same direction. The *bla*<sub>TEM-1</sub> genes in both isolates are under control of the strong P4 promoter [52], and no SNPs were detected within the promoter region or elsewhere within the plasmid.

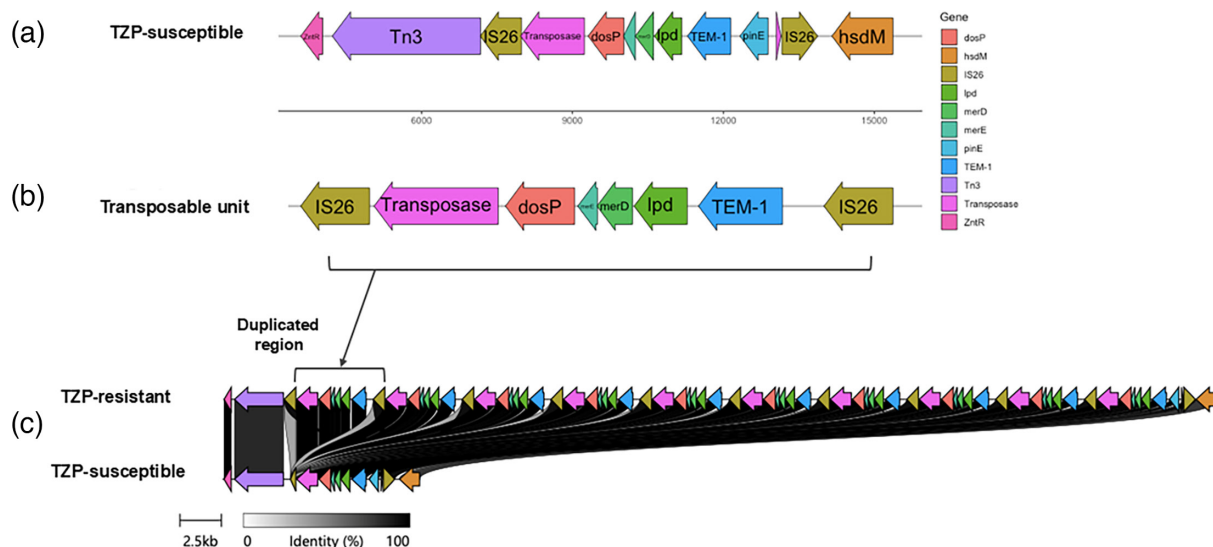


**Fig. 1.** Schematic showing (a) the location of the transposable unit within the TZP-S isolate, (b) the structure of the resistance gene cassette which was duplicated ten times in the TZP-R isolate and (c) the size and percentage identity of the duplicated region in the TZP-R isolate when compared to the TZP-S isolate. The information depicted in the schematic was determined through WGS and assembly of the respective isolates.

A comparison of the predicted resistance genes in both isolates highlighted the presence of resistances to additional drug classes (Table 1) located both on the plasmid and the chromosome. Other than duplication of *bla*<sub>TEM-1</sub>, no differences in ARGs, including resistance-conferring SNPs, were predicted when comparing the TZP-S isolate with the TZP-R isolate.

### Confirmation of increased $\beta$ -lactamase activity

Having identified the duplication of *bla*<sub>TEM-1</sub> in the TZP-R isolate, we used the nitrocefin hydrolysis assay to determine the comparative activity of  $\beta$ -lactamase. Following overnight culture of both isolates in nutrient-rich media and in the absence of TZP, a significant increase in nitrocefin hydrolysis was observed in the TZP-R isolate at the midway point of the assay ( $P < 0.001$ ), confirming increased levels of  $\beta$ -lactamase enzymatic activity (Fig. 2a, b). qPCR performed on the isolates showed increased gene copy number. The log<sub>2</sub> fold change of both *bla*<sub>TEM-1</sub> and IS26 (relative to the single-copy housekeeping gene *uidA*) was significantly increased from 0.97 to 7.05 ( $P = 0.001$ , log<sub>2</sub> fold change = -0.05 to 2.80) and 3.16 to 8.20 ( $P = 0.003$ , log<sub>2</sub> fold change = 1.66 to 2.89), respectively, in the TZP-R isolate. The slight increase in *repA* copy number from 1.24 to 1.83 ( $P = 0.047$ , log<sub>2</sub> fold change = 0.31 to 0.85) in the TZP-R isolate, compared to the TZP-S isolate, although statistically significant, is not indicative of a substantial increase in plasmid copy number (Fig. 2c).

### Copy number of *bla*<sub>TEM-1</sub> and IS26 in response to an increasing concentration of tazobactam

We aimed to determine if increasing the concentration of tazobactam, whilst fixing the piperacillin at the breakpoint ( $8 \mu\text{g ml}^{-1}$ ), led to a change in *bla*<sub>TEM-1</sub>, IS26 and *repA* copy number, as detected by qPCR. The copy number of *bla*<sub>TEM-1</sub> in the TZP-S isolate increased when the concentration of tazobactam was  $1 \mu\text{g ml}^{-1}$  or greater (Fig. 3). However, a significant increase in copy number was only observed when analysing the gene copy number change in response to  $2 \mu\text{g ml}^{-1}$ , when compared to  $0 \mu\text{g ml}^{-1}$  of tazobactam. Fold change of *bla*<sub>TEM-1</sub> compared to the single-copy housekeeping gene *uidA* increased from 0.82 to 1.44 ( $P = 0.0065$ , log<sub>2</sub> fold change = -0.31 to 2.63). The copy number of IS26 remained similar in the TZP-S isolate between tazobactam concentrations of 0 to  $1 \mu\text{g ml}^{-1}$ ; however, a statistically significant increase in the copy number of IS26 was observed with  $2 \mu\text{g ml}^{-1}$  tazobactam, where the fold change increased from 2.51 to 4.66 ( $P = 0.0067$ , log<sub>2</sub> fold change = 1.33 to 2.22). Similarly, in the TZP-R isolate, the copy number of *bla*<sub>TEM-1</sub> increased when the concentration of tazobactam was  $1 \mu\text{g ml}^{-1}$  or greater (Fig. 3), and a statistically significant increase in copy number was only observed when analysing the change in response to  $8 \mu\text{g ml}^{-1}$  and compared with  $0 \mu\text{g ml}^{-1}$  of tazobactam. Fold change of *bla*<sub>TEM-1</sub>, compared to the single-copy housekeeping gene *uidA*, increased from 6.24 to 10.95 ( $P = 0.001$ , log<sub>2</sub> fold change = 2.62 to 3.45). In the TZP-R isolate, a similar copy number of IS26 was observed across concentrations of tazobactam from 0 to  $8 \mu\text{g ml}^{-1}$ , and no significant changes in IS26 copy number were identified. The increase in *repA* copy number from 0.98 to 1.14 ( $P = 0.002$ , log<sub>2</sub> fold change = -0.03 to 0.49), observed when comparing 2 to  $0 \mu\text{g ml}^{-1}$  tazobactam, although statistically significant, does not represent a biologically relevant change in gene copy number. No significant change was observed in the TZP-R isolate in response to any increase in tazobactam concentration (Fig. S4).

**Table 1.** The TZP-S and TZP-R isolates had the same predicted repertoire of ARGs; the only exception was the number of copies of *bla*<sub>TEM-1</sub>; one copy was found in the TZP-S isolate, whereas ten copies were found in the TZP-R isolate. RGI was used to identify genes from WGS data using the CARD database; only genes designated as perfect hits (100% sequence identity and coverage) are shown

Resistance gene/mutation	Location	Drug class
<i>bla</i> <sub>TEM-1</sub>	Translocatable unit	$\beta$ -Lactam
<i>aadA5</i>	Plasmid	Aminoglycoside
<i>qacEdelta1</i>	Plasmid	Antiseptics/disinfectants
<i>sul1</i>	Plasmid	Sulphonamide
<i>Mrx</i>	Plasmid	Macrolide
<i>mphA</i>	Plasmid	Macrolide
<i>evgA</i>	Chromosome	Macrolide, fluoroquinolone, penam, tetracycline
<i>baeR</i>	Chromosome	Aminoglycoside, aminocoumarin
<i>H-NS</i>	Chromosome	Macrolide, fluoroquinolone, $\beta$ -lactam, tetracycline
<i>mdtH</i>	Chromosome	Fluoroquinolone
<i>leuO</i>	Chromosome	Nucleoside, antiseptics/disinfectants
<i>gadW</i>	Chromosome	Macrolide, fluoroquinolone, penam, tetracycline
<i>cpxA</i>	Chromosome	Aminoglycoside, aminocoumarin

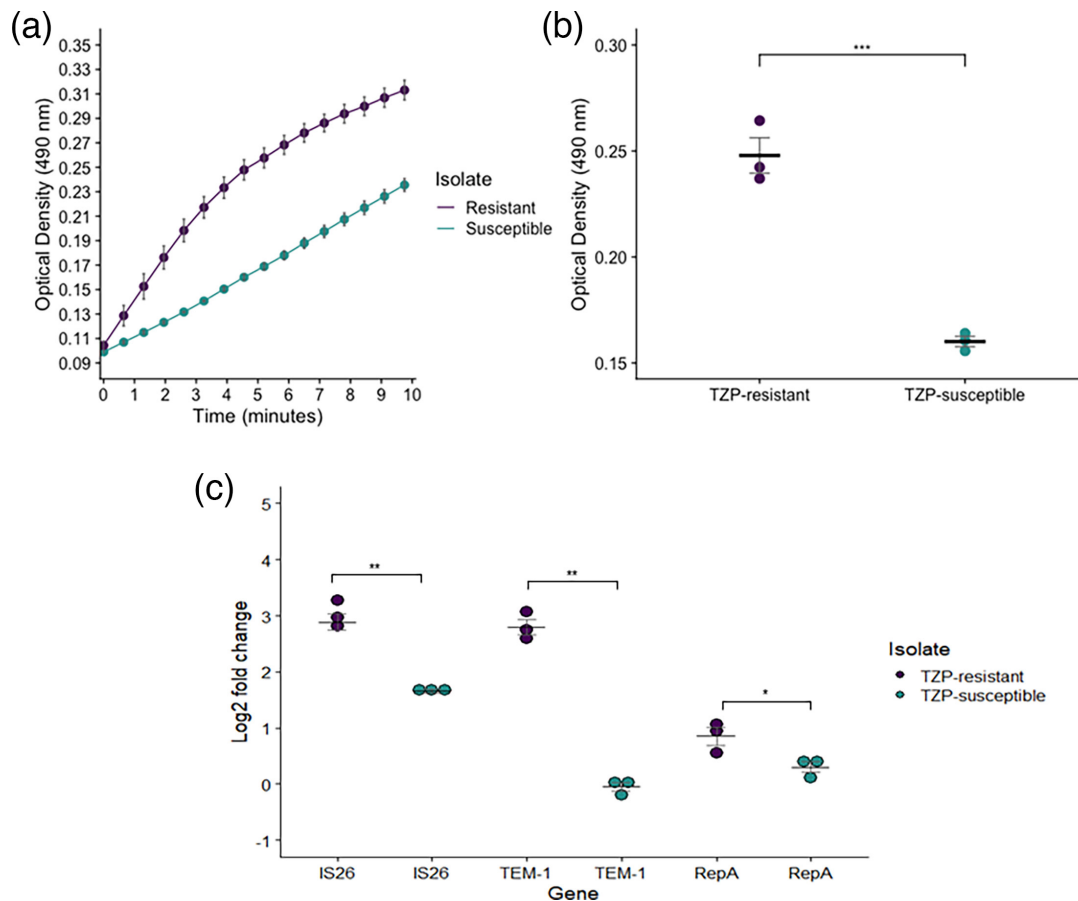


**Fig. 2.** Nitrocefin hydrolysis measured at OD<sub>490</sub> was greatest in the TZIP-R isolate (purple points/line) (a) throughout the assay and significantly increased (b) at the middle time point of the assay when compared to the TZIP-S isolate (green points/line). (c) qPCR performed showed an increase in gene copy number of both *bla*<sub>TEM-1</sub> and IS26 in the TZIP-R isolate when compared to the TZIP-S isolate, following normalization against *uidA*, a single-copy housekeeping gene. In both experiments, three biological repeats using distinct bacterial colonies were performed, and each measurement was made up of three technical repeats. In (a), points show the mean of the three biological repeats, which had been determined from the technical repeats. In (b) and (c), each point shows an individual biological repeat; the black horizontal line shows the mean of the biological repeats. In all cases, error bars show the SEM. Statistical significance in (b) and (c) was calculated using an unpaired t-test. For (c), non-transformed copy number estimates were used to determine statistical significance. \*\*= $P \leq 0.01$ , \*\*\*= $P \leq 0.001$ .

### Copy number of *bla*<sub>TEM-1</sub> and IS26 in response to an increasing concentration of piperacillin

As the TZIP-R isolate survived in concentrations of piperacillin up to and  $>256 \mu\text{g ml}^{-1}$ , we investigated the relationship between increasing piperacillin concentration and the copy number of *bla*<sub>TEM-1</sub> and IS26 whilst fixing the concentration of the inhibitor. Overall, copy numbers of both *bla*<sub>TEM-1</sub> and IS26 did increase in response to an increasing concentration of piperacillin (Fig. 4). However, a statistically significant increase in gene copy number was only observed when analysing the gene copy number change in response to  $256 \mu\text{g ml}^{-1}$ , when compared with  $0 \mu\text{g ml}^{-1}$  of piperacillin. When comparing these conditions, the fold change of *bla*<sub>TEM-1</sub> and IS26 compared to the single-copy housekeeping gene *uidA* increased from 9.47 to 53.95 ( $P \leq 0.01$ , log<sub>2</sub> fold change=3.22 to 5.58) and 8.83 to 38.21 ( $P < 0.01$ , log<sub>2</sub> fold change=3.12 to 5.17), respectively. This indicates a step change of gene copy number rather than a gradual increase in response to increasing piperacillin concentration.

### Copy number of *bla*<sub>TEM-1</sub> and IS26 remains stable in the TZIP-R isolate for a period of 5 days in the absence of TZP

To investigate the stability of the amplification of *bla*<sub>TEM-1</sub> and IS26 and whether it was sustained over multiple daily passages, we determined their copy number over 5 days with daily sampling and qPCR. This was measured both in the presence or absence of selection pressure (CA-MHB-2 supplemented with TZP or without, respectively) and in a nutrient-limited (MM) environment (Fig. 5). Gene copy number of both *bla*<sub>TEM-1</sub> and IS26 was highest in the TZIP-R isolate when cultured in CA-MHB-2 supplemented with TZP. In the presence of TZP, there was an increase in gene copy number of *bla*<sub>TEM-1</sub> and IS26 from day 1 to day 2, which was sustained until day 5 (Table 2). In the absence of TZP, gene copy number remained stable, with no significant change in

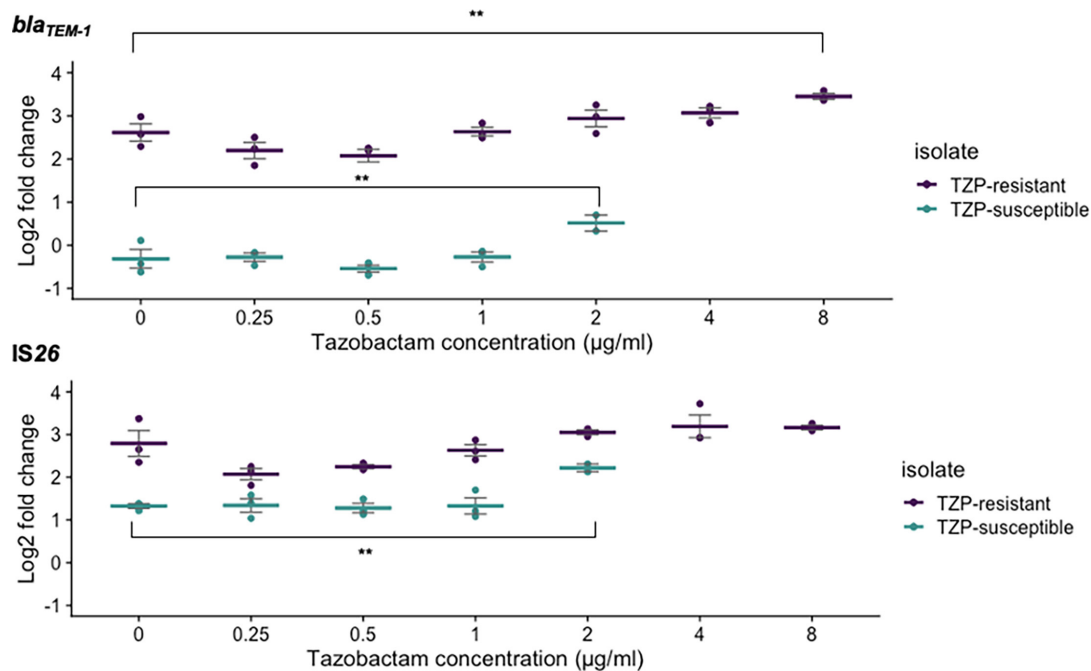


**Fig. 3.** qPCR performed following the culture of isolates in an increasing concentration of tazobactam showed that the gene copy number of *bla*<sub>TEM-1</sub> in both the TZP-S (green points/dashes) and TZP-R (purple points/dashes) isolates was greatest when the concentration of tazobactam was also greatest. A significant increase in IS26 copy number was only detected in the TZP-S (green points/dashes) isolate when the tazobactam concentration was 2 µg ml<sup>-1</sup>. The TZP-S isolate was not able to survive at concentrations of tazobactam which exceeded 2 µg ml<sup>-1</sup>. The concentration of piperacillin was fixed at 8 µg ml<sup>-1</sup>, and *bla*<sub>TEM-1</sub> and IS26 copy number and fold change were calculated following normalization against *uidA*, a single-copy housekeeping gene. Each point shows one biological repeat, and each dash shows the mean of the three biological repeats. Error bars show the SEM. Graphs showing each biological repeat in isolation can be found in Fig. S5. Statistical analysis was performed on non-transformed copy number estimates using ANOVA and Dunnett's post-hoc test using 0 µg ml<sup>-1</sup> of tazobactam as the control group. \*\*=*P*≤0.01.

either *bla*<sub>TEM-1</sub> or IS26, on any day during the experiment, compared to day 1. This indicates that the removal of selection does not readily reverse this amplification and the resistance phenotype. This is also consistent with the lack of a measurable growth fitness cost of TZP-R compared to TZP-S.

### Investigation into other genes duplicated within the resistance transposable unit

We next explored the effect of the duplication of other genes in the TZP-R duplicated transposable unit, in particular *dosP* and *lpd*. The co-amplification of these genes with ARGs, facilitated by mobile genetic elements (MGEs), has not previously been described. *DosP* is a well-characterized phosphodiesterase, which is usually encoded as part of the *dosCP* operon and regulates cellular levels of the secondary messenger, c-di-GMP, by hydrolysing it to linear-di-GMP [53, 54], which is implicated in controlling biofilm formation and swimming motility [55]. However, though *dosP* was duplicated ten-fold in the TZP-R isolate, we found no significant difference in either motility (supplementary methods and Fig. S7A) or biofilm production (supplementary methods and Fig. S7B) when comparing the two isolates and no change in the *dosCP* operon on the chromosome.

The Congo red assay (supplementary methods), which differentially stains extracellular matrix components in live cells, highlighted a visual difference in morphology when comparing the two isolates (Fig. S8). Following 24 h growth, the TZP-S isolate had bound very little of the dye, and colonies appeared pale white/cream in colour (Fig. S8A). In contrast, the TZP-R isolate had taken up the dye, and colonies were predominantly dark red in colour and had a distinctive star-like pattern, with lines radiating out from the centre of the colonies, which previous studies have indicated occur due to cellulose production [56, 57]. As *dosP* decreases c-di-GMP levels, and c-di-GMP stimulates cellulose synthesis, increased expression of *dosP* should reduce cellulose production [54, 58, 59], thus contradicting the morphotype we observed. Upon reviewing the SNP analysis, we did not find supporting evidence of SNPs which may alter the production of cellulose and could not find a genomic basis for the morphotype.

Along with *dosP*, *lpd*, which encodes dihydroloipoamide dehydrogenase (LPD), was also duplicated ten-fold. LPD is critically important for the regulation of *E. coli* metabolism in anaerobic conditions [60–62], so we assessed the growth of the two isolates under anaerobic conditions. However, we found no significant difference in growth following incubation on either M9 agar or MHA in anaerobic conditions (Fig. S9).

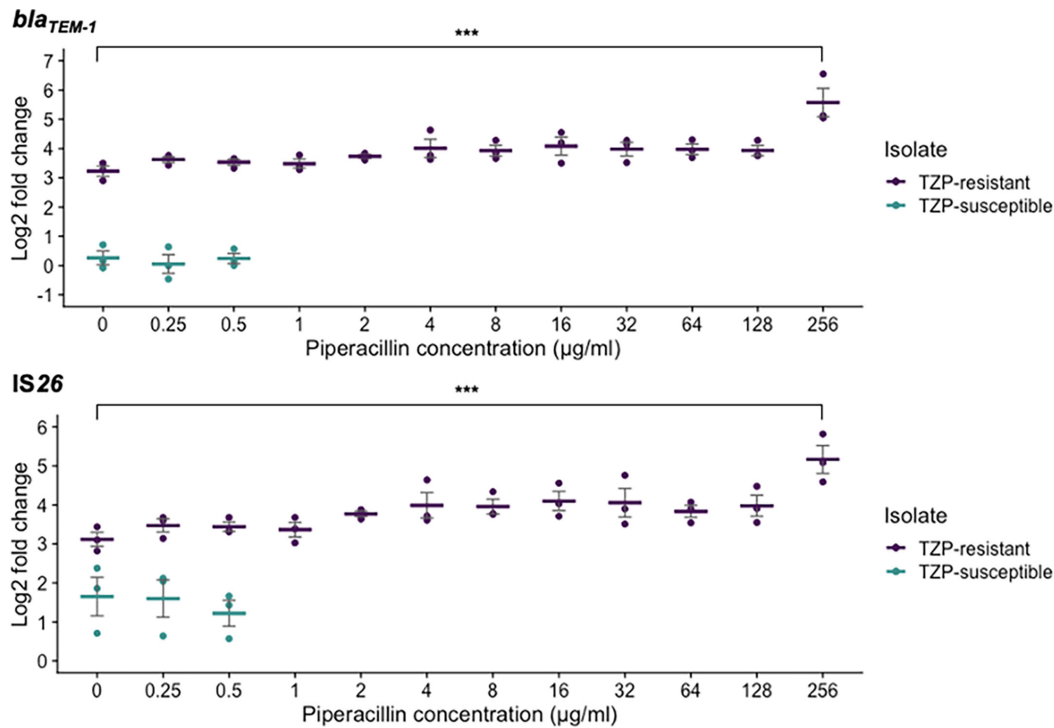


**Fig. 4.** qPCR performed following the culture of isolates in an increasing concentration of piperacillin showed that the gene copy number of both *bla*<sub>TEM-1</sub> and IS26 in the TZP-R (purple points/dashes) isolate was greatest when the concentration of piperacillin was also greatest. The TZP-S isolate (green points/dashes) was not able to survive at concentrations of piperacillin which exceeded 0.5 µg ml<sup>-1</sup>. However, when the concentration of piperacillin was 0, 0.25 or 0.5 µg ml<sup>-1</sup>, a significant increase in copy number of *bla*<sub>TEM-1</sub> and IS26 was detected in the TZP-R isolate. The concentration of tazobactam was fixed at 4 µg ml<sup>-1</sup>, and *bla*<sub>TEM-1</sub> and IS26 copy number and fold change were calculated following normalization against *uidA*, a single-copy housekeeping gene. Each point shows one biological repeat, and each dash shows the mean of the three biological repeats. Error bars show the SEM. Graphs showing each biological repeat in isolation can be found in Fig. S6. Statistical analysis was performed on non-transformed copy number estimates using ANOVA and Dunnett's post-hoc test using 0 µg ml<sup>-1</sup> of piperacillin as the control group. \*\*\*=*P*≤0.001.

Following previous unsuccessful attempts to identify a phenotype change linked to the amplification of *dosP* and *lpd*, we conducted a broad screening to assess the isolates' ability to utilize different carbon and nitrogen sources. No significant differences were observed between the TZP-S and TZP-R isolates in the carbon utilization assay (PM1) (Fig. S10). Similarly, no meaningful differences were found between the TZP-S and TZP-R isolates in the nitrogen utilization assay (PM3b) (Fig. S11). However, due to the variance observed between biological replicates (Figs S10, S12 and S14 and Figs S11, S13 and S15, respectively) for some of the tested compounds, we were unable to confidently establish average growth curves in response to those compounds.

## DISCUSSION

We performed comparative genome sequence and phenotype analyses on two patient-derived isolates that underwent within-patient evolution during antimicrobial treatment. We confirmed that the >100-fold difference in MIC to T'ZP between the isolates at the beginning and after several days of antimicrobial treatment, respectively, is driven by *bla*<sub>TEM-1</sub> duplication on a distinct translocatable unit and subsequent enzyme hyperproduction. This effect is not driven by an increase in plasmid copy number. We observed that ten copies of *bla*<sub>TEM-1</sub> are sufficient to induce this high level of enzyme production and resistance to T'ZP, but that susceptibility to 3GCs and carbapenems is retained. We also found that the culture of the TZP-R bacteria in high levels of piperacillin or tazobactam both further increased the copy number of *bla*<sub>TEM-1</sub>. Like other studies [13–15], we found that the extensive amplification of *bla*<sub>TEM-1</sub> was mediated by IS26 elements. The transmissible nature of IS26 plays a key role in the dissemination of AMR genes [63], and the location of the transposable unit on a plasmid also highlights the potential for both intraspecies and interspecies movement of *bla*<sub>TEM-1</sub>. Furthermore, transposase-mediated IS insertion may be stimulated by the presence of antimicrobials, further facilitating the emergence of clinical resistance [64]. Recent reports have characterized the amplification of *bla*<sub>SHV-5</sub> [65], inducing resistance to 3GCS, and *bla*<sub>CMY-146</sub> [66] and *bla*<sub>CTX-M-15</sub>, inducing resistance to carbapenems [67].

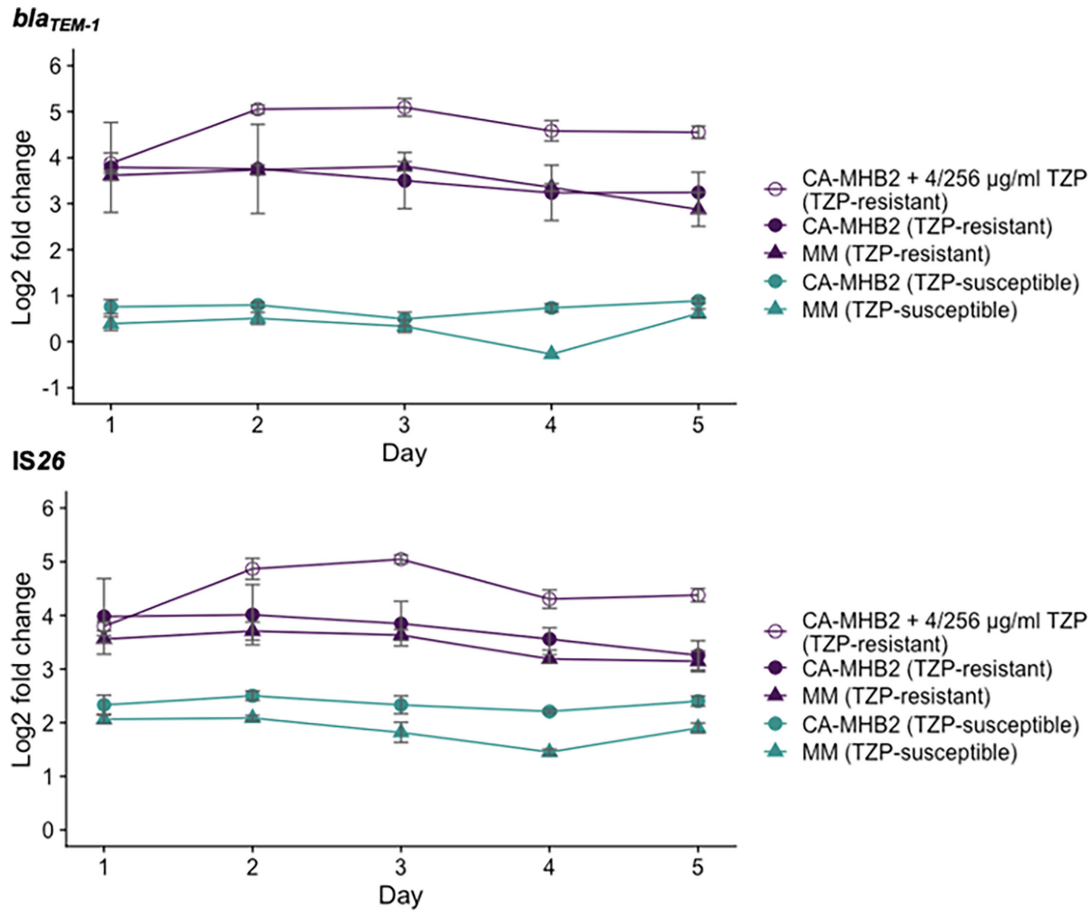


**Fig. 5.** qPCR performed following the passage of isolates every 24 h, over a period of 5 days, showed that the gene copy number of both *bla<sub>TEM-1</sub>* and IS26 in the TZP-R (purple) isolate was greatest when MHB was supplemented with TZP (open purple circles). In both the TZP-R isolate and the TZP-S (green) isolate, the copy number of both *bla<sub>TEM-1</sub>* and IS26 remained stable over the experimental period. Copy number and fold change of *bla<sub>TEM-1</sub>* and IS26 were calculated following normalization against *uidA*, a single-copy gene. Each point shows the mean of three biological repeats. Error bars show the SEM.

There are conflicting data which describe the fitness cost associated with TEM-1 hyperproduction when induced by gene duplication [13, 14]. We found that the gene copy number of *bla<sub>TEM-1</sub>* and IS26 was stable over a period of 5 days, even in the absence of selection pressure. In this study, the TZP-R isolate contained an additional 48,195 bp within the plasmid compared to the TZP-S isolate, including multiple additional coding sequences. However, when comparing the growth dynamics of the two isolates, we did not find a metabolic cost associated with replicating an enlarged plasmid, as the growth curves of the two isolates were comparable. However, we acknowledge that this is a simplistic model which is unlikely to replicate the environment within a

**Table 2.** Gene copy number increase of *bla<sub>TEM-1</sub>* and IS26 in the presence of 4/256 µg ml<sup>-1</sup> TZP. The TZP-R isolate was passaged in fresh MHB+4/256 µg ml<sup>-1</sup> TZP every 24 h for a period of 5 days. Copy number was estimated from qPCR and calculated following normalization against *uidA*, a single-copy gene. Statistical analysis was performed on non-transformed gene copy number estimates using ANOVA and Dunnett's post-hoc test, using day 1 as the control group

Day	A <i>bla<sub>TEM-1</sub></i>		Day	B IS26	
	Gene copy number increase	P value		Gene copy number increase	P value
1-2	18.26	<0.01	1-2	15.8	<0.01
1-3	19.66	<0.01	1-3	19.2	<0.001
1-4	9.46	NS	1-4	6.09	NS
1-5	8.6	NS	1-5	6.98	NS

human host. We only confirmed the increased copy number of  $bla_{\text{TEM-1}}$  and IS26. It is possible that the additional duplicated genes located on the transposable unit were not expressed at high levels; however, it is also plausible that the metabolism-linked *lpd* gene duplicated via IS26 as part of the  $bla_{\text{TEM-1}}$  cassette provided a compensatory fitness advantage to the TZP-R isolate, but detailed investigation of this goes beyond this study.

Another gene duplicated as part of the IS26-induced  $bla_{\text{TEM-1}}$  cassette amplification was *DosP*. We note that *DosP* has a role in c-di-GMP metabolism, a complex key regulator of many other cellular processes, including growth [53], stress adaptation [68], persistence [69] and virulence [55]; in particular, the observation of increased persistence of *E. coli* in ampicillin and ciprofloxacin following overexpression of *DosP* [61], which could be driven by the extensive duplications of *dosP* we observed in the resistant isolate. We could not find any significant difference in motility or biofilm production, two processes regulated by *DosC* and *DosP*, which might be due to the low numbers of *DosC* compared to *DosP* in the resistant isolate. As we did not quantify the ratio of c-di-GMP to linear-di-GMP, we cannot be sure that the extensive duplication of *dosP* resulted in increased c-di-GMP hydrolysis.

The morphology of the TZP-R isolate on Congo red agar was markedly different from the TZP-S isolate; whilst the colonies did not appear 'rough' on visualization, there were marked similarities with the 'pink/red, dry and rough' (rdar and pdar) morphotype observed in other *Enterobacteriales*. Rdar morphology has been reported in *Salmonella* [70], *E. coli* [55, 56] and *Klebsiella pneumoniae* [71] and is associated with increased cellulose expression, which can improve bacterial persistence in adverse environmental conditions and is understood as a step in adaptation to the human host [72]. Confirmatory experiments are needed; however, we hypothesize that the morphology of the TZP-R isolate may be due to increased cellulose expression, though we are currently unable to find a genomic explanation for this. Our study further emphasizes the relevance of better understanding and trying to prevent resistance phenotype evolution as a result of antimicrobial treatment, as the evolutionary pressure can lead to the selection of not only more resistant but also better host-adapted and putatively more virulent strains.

A broader assessment of carbon and nitrogen utilization yielded no meaningful findings. However, we acknowledge that the variance among replicates for the nitrogen utilization plates may have obscured subtle differences. Additionally, we did not subject the isolates to any antimicrobial selection pressure, which might have been necessary to trigger the pathways responsible for inducing a modified phenotype.

The importance of improving phenotypic-based AST, biochemical assays and utilizing predictions from genomic data is highlighted by the TZP-R/3GC-S phenotype presented in this study and the need to account for gene copy number and predicted expression levels when predicting resistance to BL/BLI combinations. Scores for BL/BLI resistance prediction from genomic data have been developed [73] in addition to  $\beta$ -lactamase copy number calculators [74], and tools like these will be vital to support decisions for use of new BL/BLI combinations and ensure their future efficacy is safeguarded. Alternative diagnostic methods, based on protein detection, such as matrix-assisted laser desorption/ionization MS technology, may provide an alternative strategy to rapidly detect  $\beta$ -lactamase hyperproduction [75].

BL/BLI combinations such as TZP are an important strategy for the treatment of invasive and disseminated infections caused by *E. coli*, including those caused by *E. coli* strains expressing Ambler class A  $\beta$ -lactamases such as  $bla_{\text{TEM-1}}$  [5]. Our investigation contributes to a growing body of evidence highlighting hyperproduction of TEM-1 as a mechanism by which tazobactam use can be overcome, resulting in treatment failure. In the absence of other information, TZP treatment failure may incorrectly suggest that an isolate is an ESBL- or ampC-producing strain and promote carbapenem usage. In this study, a carbapenem was ultimately used and treatment was successful; however, it may have also been possible to successfully treat the patient with a 3GC, given that the TZP-R isolate was still susceptible to cefpodoxamine. Promoting the de-escalation of antimicrobial selection and reducing exposure to broad-spectrum antimicrobials of last resort (such as carbapenems) is vitally important to prevent the further emergence of resistance and retain viable treatment options. It is therefore imperative that alternative mechanisms of AMR, such as IS-mediated  $\beta$ -lactamase amplification, are a priority area of research, especially efforts focused on the identification of these genotypes and understanding their evolution and transmission.

#### Funding information

A.J.F. was supported by a UKRI Medical Research Council (MR/R015678/1) MRC/CASE scholarship. E.H. acknowledges funding from Wellcome (217303/Z/19/Z) and the BBSRC (BB/V011278/1, BB/V011278/2). P.A.H. is supported by the Royal Academy of Engineering Research Chair Scheme (RCSRF2021\11\15).

#### Acknowledgements

The authors would like to thank Dr Alan Cartmell for generously providing the *Bacteroides thetaiotaomicron* (VPI-5482) positive anaerobic control strain and the patient for their collaboration and enabling their research.

#### Author contributions

Conceptualization: R.B., J.J.V.A., C.M.P., E.H., T.E. Data Curation: A.J.F., R.B., J.J.V.A., C.M.P. Formal Analysis: A.J.F., R.B., J.T.M. Funding Acquisition: P.A.H., E.H., T.E. Investigation: A.J.F., R.B., D.C., L.E.B., J.T.M. Methodology: A.J.F., E.H., T.E. Project Administration: E.H., T.E. Resources: R.B., D.C., F.E.G., J.T.M., P.A.H., J.M.L., J.J.V.A., C.M.P. Software: A.J.F., E.H., T.E. Validation: A.J.F., D.C., L.E.B., J.T.M. Visualization: A.J.F. Writing – Original Draft Preparation: A.J.F. Writing – Review and Editing: A.J.F., F.E.G., P.A.H., J.T.M., C.M.P., E.H., T.E. All authors read and approved the final manuscript.

**Conflicts of interest**

The authors declare that there are no conflicts of interest.

**Ethical statement**

Both *E. coli* isolates used in this study were collected from the Royal Liverpool University Hospital (RLUH; Liverpool, UK), as part of routine clinical diagnostic procedures. Informed consent was obtained from the patient to publish case details and carry out experimental work, and the study was approved by the Liverpool School of Tropical Medicine Research Ethics Committee (study no. 22-074). Isolates were retrieved from the hospital biobank under a Material Transfer Agreement between Liverpool Clinical Laboratories (LCL) and LSTM.

**References**

- Bush K, Bradford PA.  $\beta$ -Lactams and  $\beta$ -lactamase inhibitors: an overview. *Cold Spring Harb Perspect Med* 2016;6:a025247.
- National institute for health care excellence (NICE). British National Formulary Treatment Summaries: cephalosporins; 2023. <https://bnf.nice.org.uk/treatment-summaries/cephalosporins/>
- National institute for health care excellence (NICE). British National Formulary Treatment Summaries: carbapenems; 2023. <https://bnf.nice.org.uk/treatment-summaries/carbapenems>
- Murray CJ, Ikuta KS, Sharara F, Swetschinski L, Aguilar GR, et al. Global burden of bacterial antimicrobial resistance in 2019: a systematic analysis. *Lancet* 2022;399:629–655.
- Barton GJ, Morecroft CW, Henney NC. A survey of antibiotic administration practices involving patients with sepsis in UK critical care units. *Int J Clin Pharm* 2020;42:65–71.
- Wilson APR. Sparing carbapenem usage. *J Antimicrob Chemother* 2017;72:2410–2417.
- Suzuki Y, Sato T, Fukushima Y, Nakajima C, Suzuki Y, et al. Contribution of  $\beta$ -lactamase and efflux pump overproduction to tazobactam-piperacillin resistance in clinical isolates of *Escherichia coli*. *Int J Antimicrob Agents* 2020;55:105919.
- Crowley B, Benedí VJ, Doménech-Sánchez A. Expression of SHV-2  $\beta$ -lactamase and of reduced amounts of OmpK36 porin in *Klebsiella pneumoniae* results in increased resistance to cephalosporins and carbapenems. *Antimicrob Agents Chemother* 2002;46:3679–3682.
- Sanbongi Y, Suzuki T, Osaki Y, Senju N, Ida T, et al. Molecular evolution of  $\beta$ -lactam-resistant *Haemophilus influenzae*: 9-year surveillance of penicillin-binding protein 3 mutations in isolates from Japan. *Antimicrob Agents Chemother* 2006;50:2487–2492.
- Lee J, Oh CE, Choi EH, Lee HJ. The impact of the increased use of piperacillin/tazobactam on the selection of antibiotic resistance among invasive *Escherichia coli* and *Klebsiella pneumoniae* isolates. *Int J Infect Dis* 2013;17:e638–43.
- van Duin D, Bonomo RA. Ceftazidime/avibactam and ceftolozane/tazobactam: second-generation  $\beta$ -lactam/ $\beta$ -lactamase inhibitor combinations. *Clin Infect Dis* 2016;63:234–241.
- Turner MS, Andersson P, Bell JM, Turnidge JD, Harris T, et al. Plasmid-borne blaSHV genes in *Klebsiella pneumoniae* are associated with strong promoters. *J Antimicrob Chemother* 2009;64:960–964.
- Hubbard A, Mason J, Roberts P, Parry CM, Corless C, et al. Piperacillin/tazobactam resistance in a clinical isolate of *Escherichia coli* due to IS26-mediated amplification of blaTEM-1B. *Nat Commun* 2020;11:4915.
- Hansen KH, Andreasen MR, Pedersen MS, Westh H, Jelsbak L, et al. Resistance to piperacillin/tazobactam in *Escherichia coli* resulting from extensive IS26-associated gene amplification of blaTEM-1. *J Antimicrob Chemother* 2019;74:3179–3183.
- Schechter LM, Creely DP, Garner CD, Shortridge D, Nguyen H, et al. Extensive gene amplification as a mechanism for piperacillin-tazobactam resistance in *Escherichia coli*. *mBio* 2018;9:e00583–18.
- San Millan A, Escudero JA, Gifford DR, Mazel D, MacLean RC. Multi-copy plasmids potentiate the evolution of antibiotic resistance in bacteria. *Nat Ecol Evol* 2016;1:1–8.
- Rosenkilde CE, Munck C, Porse A, Linkevicius M, Andersson DI, et al. Collateral sensitivity constrains resistance evolution of the CTX-M-15  $\beta$ -lactamase. *Nat Commun* 2019;10:618.
- Edwards T, Heinz E, van Aartsen J, Howard A, Roberts P, et al. Piperacillin/tazobactam resistant, cephalosporin susceptible *Escherichia coli* bloodstream infections are driven by multiple acquisition of resistance across diverse sequence types. *Microbiology* 2020. DOI: 10.1101/2020.09.18.302992.
- Maillard A, Delory T, Bernier J, Villa A, Chaibi K, et al. Effectiveness of third-generation cephalosporins or piperacillin compared with cefepime or carbapenems for severe infections caused by wild-type AmpC  $\beta$ -lactamase-producing *Enterobacterales*: a multi-centre retrospective propensity-weighted study. *Int J Antimicrob Agents* 2023;62:106809.
- Harris PN, Tambyah PA, Lye DC, Mo Y, Lee TH, et al. Effect of piperacillin-tazobactam vs meropenem on 30-day mortality for patients with *E. coli* or *Klebsiella pneumoniae* bloodstream infection and ceftriaxone resistance: a randomized clinical trial. *JAMA* 2018;320:984–994.
- Kahlmeter G, Brown D, Goldstein F, MacGowan A, Mouton R, et al. European committee on antimicrobial susceptibility testing (EUCAST) technical notes on antimicrobial susceptibility testing. *Clin Microbiol Infect* 2006;12:501–503.
- The European Committee on Antimicrobial Susceptibility Testing. Breakpoint tables for the interpretation of MICs and zone diameters. Version 10.0; 2020. [www.eucast.org](http://www.eucast.org)
- Bolger AM, Lohse M, Usadel B. Trimmomatic: a flexible trimmer for Illumina sequence data. *Bioinformatics* 2014;30:2114–2120.
- Andrews S. FastQC: a quality control tool for high throughput sequence data. Cambridge, United Kingdom: Babraham Bioinformatics, Babraham Institute; 2010.
- Oxford Nanopore Technologies. Guppy; (n.d.). <https://community.nanoporetech.com/downloads>
- Wick RR, Menzel P. Filtlong; 2017. <https://github.com/rrwick/Filtlong>
- Wick R. Porechop: adapter trimmer for Oxford Nanopore reads; 2018. <https://github.com/rrwick/Porechop>
- Wick RR, Judd LM, Gorrie CL, Holt KE. Unicycler: resolving bacterial genome assemblies from short and long sequencing reads. *PLoS Comput Biol* 2017;13:e1005595.
- Wick RR, Schultz MB, Zobel J, Holt KE. Bandage: interactive visualization of *de novo* genome assemblies. *Bioinformatics* 2015;31:3350–3352.
- Oxford Nanopore Technologies. Medaka; (n.d.). <https://github.com/nanoporetech/medaka>
- Wick RR, Holt KE. Polypolish: short-read polishing of long-read bacterial genome assemblies. *PLoS Comput Biol* 2022;18:e1009802.
- Hu J, Fan J, Sun Z, Liu S. NextPolish: a fast and efficient genome polishing tool for long-read assembly. *Bioinformatics* 2020;36:2253–2255.
- Li H. Aligning sequence reads, clone sequences and assembly contigs with BWA-MEM. 13033997. arXiv preprint arXiv 2013.
- Li H, Handsaker B, Wysoker A, Fennell T, Ruan J, et al. The sequence alignment/map format and SAMtools. *bioinformatics* 2009;25:2078–2079.
- Rutherford K, Parkhill J, Crook J, Horsnell T, Rice P, et al. Artemis: sequence visualization and annotation. *Bioinformatics* 2000;16:944–945.
- Carver TJ, Rutherford KM, Berriman M, Rajandream M-A, Barrell BG, et al. ACT: the artemis comparison tool. *Bioinformatics* 2005;21:3422–3423.

37. Seemann T. Prokka: rapid prokaryotic genome annotation. *Bioinformatics* 2014;30:2068–2069.
38. Maiden MC, Bygraves JA, Feil E, Morelli G, Russell JE, et al. Multi-locus sequence typing: a portable approach to the identification of clones within populations of pathogenic microorganisms. *Proc Natl Acad Sci USA* 1998;95:3140–3145.
39. Joensen KG, Tetzschner AM, Iguchi A, Aarestrup FM, Scheutz F. Rapid and easy in silico serotyping of *Escherichia coli* isolates by use of whole-genome sequencing data. *J Clin Microbiol* 2015;53:2410–2426.
40. Lee I, Ouk Kim Y, Park S-C, Chun J. OrthoANI: an improved algorithm and software for calculating average nucleotide identity. *Int J Syst Evol Microbiol* 2016;66:1100–1103.
41. Carattoli A, Zankari E, García-Fernández A, Voldby Larsen M, Lund O, et al. In silico detection and typing of plasmids using PlasmidFinder and plasmid multilocus sequence typing. *Antimicrob Agents Chemother* 2014;58:3895–3903.
42. Bortolaia V, Kaas RS, Ruppe E, Roberts MC, Schwarz S, et al. ResFinder 4.0 for predictions of phenotypes from genotypes. *J Antimicrob Chemother* 2020;75:3491–3500.
43. Alcock BP, Huynh W, Chalil R, Smith KW, Raphenya AR, et al. CARD 2023: expanded curation, support for machine learning, and resistance prediction at the comprehensive antibiotic resistance database. *Nucleic Acids Res* 2023;51:D690–D699.
44. Deatherage DE, Barrick JE. Identification of mutations in laboratory-evolved microbes from next-generation sequencing data using breseq. *Methods Mol Biol* 2014;1151:165–188.
45. Livak KJ, Schmittgen TD. Analysis of relative gene expression data using real-time quantitative PCR and the 2(-Delta Delta C(T)) Method. *Methods* 2001;25:402–408.
46. Edwards T, Williams C, Teethaisong Y, Sealey J, Sasaki S, et al. A highly multiplexed melt-curve assay for detecting the most prevalent carbapenemase, ESBL, and AmpC genes. *Diagn Microbiol Infect Dis* 2020;97:115076.
47. Edwards T, Sasaki S, Williams C, Hobbs G, Feasey NA, et al. Speciation of common gram-negative pathogens using a highly multiplexed high resolution melt curve assay. *Sci Rep* 2018;8:1114.
48. R Core Team. R: a language and environment for statistical computing. R Foundation for Statistical Computing, Vienna, Austria; (n.d.). <https://www.R-project.org>
49. Villanueva RAM, Chen ZJ. ggplot2: elegant graphics for data analysis. Taylor & Francis, 2019.
50. Wilkins D. Gggenes: draw gene arrow maps in "ggplot2". R package version 0.5.0, 2023.
51. Team RC. R: a language and environment for statistical computing. 2013.
52. Zhou K, Tao Y, Han L, Ni Y, Sun J. Piperacillin-tazobactam (TZP) resistance in *Escherichia coli* due to hyperproduction of TEM-1  $\beta$ -lactamase mediated by the promoter Pa/Pb. *Front Microbiol* 2019;10:833.
53. Römbling U, Galperin MY, Gomelsky M. Cyclic di-GMP: the first 25 years of a universal bacterial second messenger. *Microbiol Mol Biol Rev* 2013;77:1–52.
54. Tuckerman JR, Gonzalez G, Sousa EHS, Wan X, Saito JA, et al. An oxygen-sensing diguanylate cyclase and phosphodiesterase couple for c-di-GMP control. *Biochemistry* 2009;48:9764–9774.
55. Cimdins A, Simm R, Li F, Lühje P, Thorell K, et al. Alterations of c-di-GMP turnover proteins modulate semi-constitutive rdar biofilm formation in commensal and uropathogenic *Escherichia coli*. *Microbiologyopen* 2017;6:e00508.
56. Bokranz W, Wang X, Tschäpe H, Römbling U. Expression of cellulose and curli fimbriae by *Escherichia coli* isolated from the gastrointestinal tract. *J Med Microbiol* 2005;54:1171–1182.
57. Lajhar SA, Brownlie J, Barlow R. Characterization of biofilm-forming capacity and resistance to sanitizers of a range of *E. coli* O26 pathotypes from clinical cases and cattle in Australia. *BMC Microbiol* 2018;18:41.
58. Ross P, Weinhouse H, Aloni Y, Michaeli D, Weinberger-Ohana P, et al. Regulation of cellulose synthesis in *Acetobacter xylinum* by cyclic diguanylic acid. *Nature* 1987;325:279–281.
59. Richter AM, Possling A, Malysheva N, Yousef KP, Herbst S, et al. Local c-di-GMP signaling in the control of synthesis of the *E. coli* biofilm exopolysaccharide pEtN cellulose. *J Mol Biol* 2020;432:4576–4595.
60. Quail M, Haydon D, Guest J. The pdhR-aceEF-lpd operon of *Escherichia coli* expresses the pyruvate dehydrogenase complex. *Mol Microbiol* 1994;12:95–104.
61. Steiert P, Stauffer L, Stauffer G. The lpd gene product functions as the L protein in the *Escherichia coli* glycine cleavage enzyme system. *J Bacteriol* 1990;172:6142–6144.
62. Kim Y, Ingram L, Shanmugam K. Dihydropyrimidine dehydrogenase mutation alters the NADH sensitivity of pyruvate dehydrogenase complex of *Escherichia coli* K-12. *J Bacteriol* 2008;190:3851–3858.
63. Harmer CJ, Moran RA, Hall RM. Movement of IS26-associated antibiotic resistance genes occurs via a translocatable unit that includes a single IS26 and preferentially inserts adjacent to another IS26. *mBio* 2014;5:e01801-14.
64. Pedró L, Baños RC, Aznar S, Madrid C, Balsalobre C, et al. Antibiotics shaping bacterial genome: deletion of an IS91 flanked virulence determinant upon exposure to subinhibitory antibiotic concentrations. *PLoS One* 2011;6:e27606.
65. Zienkiewicz M, Kern-Zdanowicz I, Carattoli A, Gniadkowski M, Ceglowski P. Tandem multiplication of the IS26-flanked amplicon with the bla(SHV-5) gene within plasmid p1658/97. *FEMS Microbiol Lett* 2013;341:27–36.
66. Moran RA, Baomo L, Doughty EL, Guo Y, Ba X, et al. Extended-spectrum  $\beta$ -lactamase genes traverse the *Escherichia coli* populations of intensive care unit patients, staff, and environment. *Microbiol Spectr* 2023;11:e0507422.
67. Shropshire WC, Aitken SL, Pifer R, Kim J, Bhatti MM, et al. IS26-mediated amplification of blaOXA-1 and blaCTX-M-15 with concurrent outer membrane porin disruption associated with *de novo* carbapenem resistance in a recurrent bacteraemia cohort. *J Antimicrob Chemother* 2021;76:385–395.
68. Chua SL, Sivakumar K, Rybtke M, Yuan M, Andersen JB, et al. C-di-GMP regulates *Pseudomonas aeruginosa* stress response to tellurite during both planktonic and biofilm modes of growth. *Sci Rep* 2015;5:10052.
69. Kwan BW, Osbourne DO, Hu Y, Benedik MJ, Wood TK. Phosphodiesterase DosP increases persistence by reducing cAMP which reduces the signal indole. *Biotechnol Bioeng* 2015;112:588–600.
70. White A, Surette M. Comparative genetics of the rdar morphotype in *Salmonella*. *J Bacteriol* 2006;188:8395–8406.
71. Liu C, Dong N, Huang X, Huang Z, Cai C, et al. Emergence of the clinical rdar morphotype carbapenem-resistant and hypervirulent *Klebsiella pneumoniae* with enhanced adaptation to hospital environment. *Sci Total Environ* 2023;889:164302.
72. White A, Gibson D, Kim W, Kay W, Surette M. Thin aggregative fimbriae and cellulose enhance long-term survival and persistence of *Salmonella*. *J Bacteriol* 2006;188:3219–3227.
73. Shropshire WC, Amiji H, Bremer J, Anand SS, Strobe B, et al. Genetic determinants underlying the progressive phenotype of  $\beta$ -lactam/ $\beta$ -lactamase inhibitor resistance in *Escherichia coli*. *bioRxiv* 2023. DOI: 10.1101/2023.05.24.542208.
74. Jiang J, Chen L, Chen X, Li P, Xu X, et al. Carbapenemase-encoding gene copy number estimator (CCNE): a tool for carbapenemase gene copy number estimation. *Microbiol Spectr* 2022;10:e0100022.
75. Rodríguez Villodres A, Gálvez Benítez L, Arroyo MJ, Méndez G, Mancera L, et al. Ultrasensitive and rapid identification of ESRI developer- and piperacillin/tazobactam-resistant *Escherichia coli* by the MALDIptaz test. *Emerg Microbes Infect* 2022;11:2034–2044.